

# GENERATION OF PICOSECOND ELECTRON-BUNCH TRAINS WITH VARIABLE SPACING USING A MULTI-PULSE PHOTOCATHODE LASER\*

M. Conde<sup>1</sup>, W. Gai<sup>1</sup>, C. Jing<sup>1,2</sup>, R. Konecny<sup>1</sup>, W. Liu<sup>1</sup>, D. Mihalcea<sup>3</sup>,  
P. Piot<sup>3,4†</sup>, J. G. Power<sup>1</sup>, M. Rihaoui<sup>3</sup>, Z. Yusof<sup>1</sup>

<sup>1</sup> High-Energy-Physics Division, Argonne National Laboratory, Lemont, IL 60439, USA

<sup>2</sup> Euclid TechLabs, Solon, Ohio 44139, USA

<sup>3</sup> Department of Physics, Northern Illinois University, DeKalb, IL 60115, USA

<sup>4</sup> Accelerator Physics Center, Fermi National Accelerator Laboratory, Batavia, IL 60510, USA

## Abstract

We demonstrate the generation of a train of electron bunches with variable spacing at the Argonne Wakefield Accelerator. The photocathode ultraviolet laser pulse consists of a train of four pulses produced via polarization splitting using two alpha-BBO crystals. The photoemitted electron bunches are then manipulated in a horizontally-bending dogleg with variable longitudinal dispersion. A downstream vertically-deflecting cavity is then used to diagnose the temporal profile of the electron beam. The generation of a train composed of four bunches with tunable spacing is demonstrated. Such a train of bunch could have application to, e.g., the resonant excitation of wakefield in dielectric-lined structures.

## INTRODUCTION

Bunch trains consisting of microbunches separated by a few ps have potential applications in new acceleration concepts (resonant excitation of electromagnetic fields in plasma and wakefield acceleration) and accelerator-based light source (e.g. narrow-band tunable THz radiation sources). Therefore there has been an increasing effort to develop beam manipulation methods capable of producing sub-picosecond (ps) bunch train [1, 2, 3, 4]. In this paper, we explore a simple method to generate a train of bunches with variable ps separation. We experimentally demonstrate the technique at the Argonne Wakefield Accelerator (AWA).

The bunch-train-generation method explored in this paper is based on the use of a photoinjector and the production a train of laser pulses that impinges the photocathode. The photoemitted electron beam mirror the train structure from the laser. However due to correlations and collective effects the longitudinal density modulation eventually washes out but the energy modulation remains. Therefore, a dispersive section located downstream can be used to re-

cover the density modulation and control the bunch-train spacing.

## EXPERIMENTAL SETUP

The experimental implementation at the AWA is shown in Fig. 1 [5]. The accelerator incorporates a photoemission source consisting of a 1+1/2 cell rf cavity operating at  $f = 1.3$  GHz (rf gun). An ultraviolet (uv) laser beam impinges a magnesium photocathode located on the back plate of the rf gun half cell. The photoemitted electron bunch exits from the rf gun with an energy of  $\sim 8$  MeV and is accelerated by a 18-cell  $\pi/2$ -mode booster cavity to up to  $\sim 16$  MeV. The uv laser system consists of a Titanium Sapphire laser amplified with a regenerative amplifier. The infrared laser is frequency-tripled to  $\lambda = 248$  nm and can be further amplified in a single-stage Krypton Fluoride excimer amplifier.

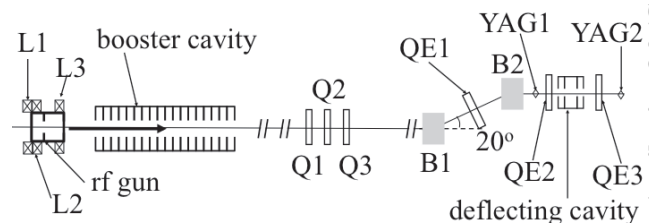


Figure 1: Overview of the experimental setup. Only subsystems relevant to this paper are shown. Q's and B's are quadrupole and dipole magnets, YAG are transverse density monitor screens, and L's are solenoidal magnetic lenses.

To produce a uv pulse train, the amplifier uv laser pulse is transmitted through a series of alpha barium borate ( $\alpha$ -BBO) birefringent crystals [6, 7]. The crystal has its optical axis making a  $45^\circ$  angle with the incident polarization resulting in a splitting of the incoming uv pulse into two pulses with orthogonal polarizations, the delay between the two pulses is given by  $\delta t = \mathcal{G}d$  where  $\mathcal{G} = -0.96$  ps/mm is the group velocity mismatch, and  $d$  the crystal thick-

\* This work was supported by DOE awards FG-02-08ER41532 with Northern Illinois University and DE-AC02-06CH11357 with Argonne National Laboratory.

† piot@nicadd.niu.edu

ness. In our experiment, a 7- and 14-mm thickness crystals were used. Passing the uv pulse through the 14-mm and then 7-mm crystals results in a train of four uv pulses with  $\delta t \sim 6.7$  ps separations [7].

After acceleration in the booster cavity, the beam propagates through a dogleg. The dogleg consists of a quadrupole (QE1) flanked by two dipole magnets (B1 and B2) with bending angles  $\pm 20^\circ$ . Such a configuration provides a variable longitudinal dispersion  $R_{56} = \int ds \eta(s)/\rho(s)$  where  $\eta(s)$  and  $\rho(s)$  are respectively the dispersion and curvature radius of the trajectory along the beamline ( $s$  is the longitudinal pathlength coordinate). For typical QE1 strengths the dogleg achieves  $R_{56} \in [-0.4, 0.1]$  m according to ELEGANT simulation [8]; see Fig. 2.

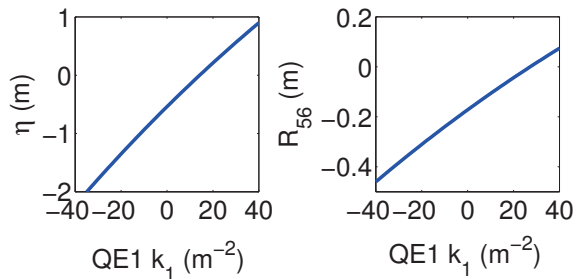


Figure 2: Simulated horizontal and longitudinal dispersion at YAG1 screen as a function of QE1 strength.

Downstream of the dogleg the beamline includes a transverse-deflecting cavity (TDC) capable of deflecting the beam in the vertical direction and two quadrupole magnets. The configuration could in principle enable single-shot longitudinal phase space measurement. In the following we only use the TDC to measure the current distribution though the dispersive (horizontal) axis is proportional to the fractional momentum spread  $\delta$ .

Given the initial 6.7-ps separation, the time-dependent accelerating fields in the rf gun and booster cavities lead to a “global” energy chirp  $\mathcal{C}$  over the train while each bunch have its own “local” chirp  $\mathcal{C}'$ . The local chirp is affected by time-dependent field and collective effect during the beam generation and low-energy transport. In applications such as, e.g., narrow-band radiation source the time separation between the bunch is critical to achieve coherent enhancement of the radiation at the desired frequency and reducing this separation to access short (e.g. THz) wavelengths is often sought. The initial spacing can be compressed by passing the beam through dispersive section with its longitudinal dispersion  $R_{56}$ . The compression factor is  $(\Delta z)/(\Delta z_0) \equiv 1 + R_{56}\mathcal{C}^{-1}$ . Practically, the minimum achievable spacing after compression is limited by the local chirp, initial root-mean square (rms) bunch length  $\sigma_0$  and initial bunch separation  $\Delta z_0$ . In particular the latter quantities should satisfy

$$\left| \frac{\Delta z_0}{\sigma_0} \right| > \left| \frac{1 + R_{56}\mathcal{C}'}{1 + R_{56}\mathcal{C}} \right|. \quad (1)$$

Therefore it is expected that going to large compression (i.e. small compression factors) would result in the bunches within the train to eventually merge.

## BEAMLINE CHARACTERIZATION

The TDC was calibrated and results pertaining to its performances are reported in Ref. [9]. A direct measurement of the  $R_{56}$  was not possible during our experiment. We therefore relied on measuring the dispersion for different values of quadrupole QE1 as an indirect way to assess, with the help of numerical simulation, the values of  $R_{56}$ .

To measure the dispersion, a standard difference-orbit measurement was implemented: given a value of QE1, the magnetic field of QE1, B1, and B2 were perturbatively changed and the corresponding horizontal position change at YAG1 and YAG2 (with magnets QE2 and QE3 off),  $\Delta x$ , was recorded. Since a change in magnetic field,  $\Delta B/B$ , is equivalent to a change in beam energy the dispersion could be computed as  $\eta = \Delta x/(\Delta B/B)$ . The measured dispersion at YAG1 and YAG2 are compared with ELEGANT simulations in Fig. 3. The simulations and experiments are observed to be in decent agreement.

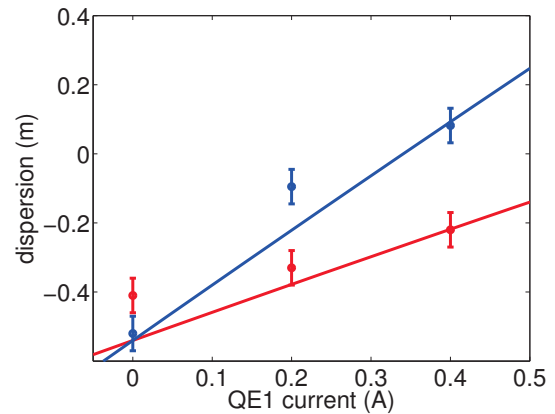


Figure 3: Simulated (lines) and measured (symbols) dispersion at YAG1 (red) and YAG2 (blue) screens.

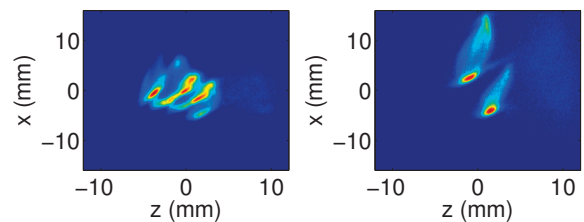


Figure 4: Spatio-temporal distribution measured at YAG2 with the 14-mm  $\alpha$ -BBO crystal (left) and the 14- and 7-mm crystals (right). The quadrupole QE1 was set to 0.5 A. The coordinate  $z$  is the longitudinal position along the bunch and  $x$  is the horizontal coordinate (which is proportional to the fractional momentum spread).

## BUNCH-TRAIN GENERATION

For the measurement reported in this Section, the total bunch charge was fixed to 0.5 nC and the beam energy was approximately 12.6 MeV. Bunch trains with either 2 or 4 bunches were generated using respectively a 14-mm crystal and a combination of a 14- and a 7-mm crystals. The generated uv pulse trains are expected to have a 13.4-ps (2 bunches) and 6.7-ps (4 bunches) separations. An example of spatio-temporal ( $z, x$ ) electron-bunch distributions measured at YAG2 for the two crystal configurations appears in Fig. 4. The apparent difference in the single-bunch beam densities arise from the charge per bunch which is twice as large for the two-bunch train compared to the four-bunch train. Therefore in the two-bunch train, the beam dynamics of the individual bunches is subject to larger to larger space-charge effects.

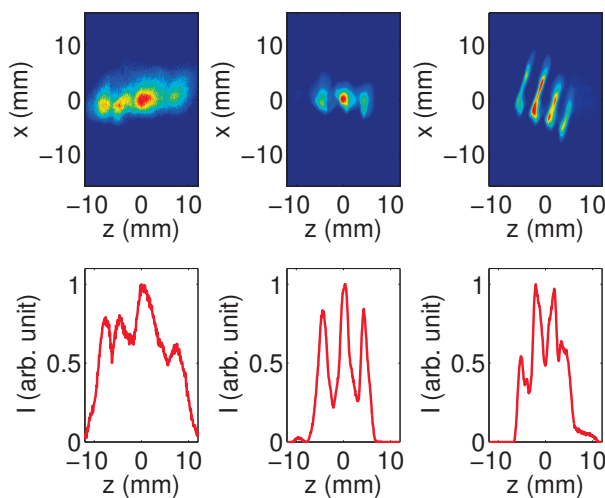


Figure 5: Measured spatio-temporal density (top row) and associated charge distribution (bottom row) at YAG2 screen for quadrupole QE1 settings of 0.2 A (left), 0.3 A (middle), and 0.4 A (right). The coordinate  $z$  is the longitudinal position along the bunch and  $x$  is the horizontal coordinate (which is proportional to the fractional momentum spread)

Altering the settings of quadrupole QE1 from 0.2 to 0.5 A enables the control of the bunch-to-bunch separation within the train as illustrated in Fig. 5. For value below 0.2 A the bunches within the train are merged into a single bunch. For value beyond 0.5 A, the beamlets have large local correlations and the modulation is attenuated; see Fig. 4 (left plot). For the settings used during our experiment, the best modulation was achieved for QE1 set to 0.3 A resulting in a bunch-to-bunch separation of  $\sim 4$  mm (or 12 ps); see Fig. 6. Although the achieved separation remains modest, the associated bunch train could be used to resonantly excite wakefield in, e.g., dielectric structures operating at  $f \sim 80$  GHz.

Finally, it is worth noting that in our experiment we did not attempt to suppress the dispersion downstream of the

dogleg. Controlling the dispersion so that it cancels at a given location, e.g., where the bunch train would need to be focused e.g. to propagate through a dielectric structure or radiate coherent radiation, can be achieved by using quadrupoles. In our configuration QE2 and QE3 could be used for such a purpose without affecting the  $R_{56}$ .

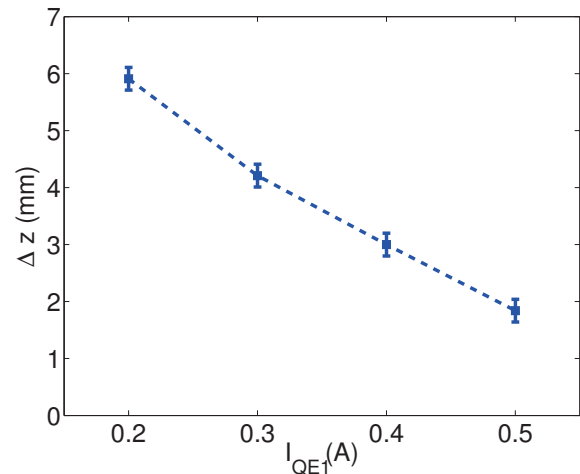


Figure 6: Measured average modulation wavelength (peaks separation  $\Delta z$ ) as a function of QE1 setting.

## SUMMARY & OUTLOOK

We have presented preliminary measurements on a simple technique to generate a train of electron bunches with variable separation. In the initial experiment appreciable density modulation down to wavelengths of  $\sim 1.8$  mm (corresponding to a temporal separation of  $\sim 6$  ps) were achieved for a total charge of 0.5 nC. Finding ways to reach smaller separations is being explored with the help of numerical simulations and will be presented elsewhere [10].

## REFERENCES

- [1] M. Bolosco, *et al.*, Nucl. Instr. Meth. **A 577**, 409 (2007).
- [2] P. Muggli, *et al.*, Phys. Rev. Lett. **101**, 054801 (2008).
- [3] Y.-E. Sun, *et al.*, Phys. Rev. Lett. **105**, 234801 (2010).
- [4] P. Piot, *et al.*, Appl. Phys. Lett. **98**, 261501 (2011).
- [5] Information on the Argonne Wakefield Facility are available at <http://gate.hep.anl.gov/awa>.
- [6] S. Zhou, *et al.*, Appl. Opt. **46**, 8488 (2007).
- [7] J. G. Power and C. Jing, AIP Conf. Proc. 1086, 689 (2009).
- [8] M. Borland, "elegant: A Flexible SDDS-Compliant Code for Accelerator Simulation", Advanced Photon Source LS-287, September 2000 (unpublished).
- [9] M. Conde, *et al.*, contribution THPPC031, these Proceedings.
- [10] J. G. Power *et al.*, to be presented at the AAC2012 workshop (2012).